Journal of Power Sources 223 (2013) 312–318

Contents lists available at SciVerse ScienceDirect

Journal of Power Sources

journal homepage: www.elsevier.com/locate/jpowsour

Short communication

A CoO_x/carbon double-layer thin film air electrode for nonaqueous Li-air batteries

Yin Yang [a,b], Qian Sun [a], Yue-Sheng Li [b], Hong Li [c], Zheng-Wen Fu [a,*]

[a] Shanghai Key Laboratory of Molecular Catalysts and Innovative Materials, Department of Chemistry & Laser Chemistry, Fudan University, Handan Road, Shanghai 200433, China
[b] Department of Materials Science, Fudan University, Shanghai 200433, China
[c] Beijing National Laboratory for Condensed Matter Physics, Institute of Physics, Chinese Academy of Sciences, Beijing 100190, China

HIGHLIGHTS

- A CoO_x/diamond like carbon (DLC) double layer thin film electrode was fabricated.
- We examined electrochemical properties of CoO_x/DLC electrode for Li-air batteries.
- CoO_x/DLC electrode exhibited a bifunctional catalytic activity for Li-air batteries.
- Spatial distribution of discharge products were investigated by SIMS.
- Bifunctional effect of CoO_x layer for Li-air battery was revealed.

ARTICLE INFO

Article history:
Received 6 April 2012
Received in revised form
25 August 2012
Accepted 15 September 2012
Available online 21 September 2012

Keywords:
Cobalt oxide/double layer electrode
Lithium air batteries
Charge–discharge profiles
Cycle ability
Secondary ion mass spectrometry

ABSTRACT

A double-layer structural air cathode consisting of diamond like carbon (DLC) active layer and CoO_x catalytic layer is designed and its catalytic effect for Li-air batteries both in carbonate and ether based electrolytes are tested. Ethylene carbonate (EC)/dimethyl carbonate (DMC) based Li-air cell using this double-layer electrode as air cathode exhibits significant improvement in discharge/charge electrochemical performance but suffers from electrolyte decomposition as proved by Fourier transform infrared (FTIR) and secondary ion mass spectrometry (SIMS) measurements. In 1,2-dimethoxyethane (DME) based electrolyte, CoO_x/DLC double layer electrode shows high catalytic activity towards oxygen evolution reaction (OER). Furthermore, over 30 cycles is achieved with a capacity of more than 2000 mAh g^{-1} by using CoO_x/DLC double layer electrode, which makes it a promising air electrode for Li-air batteries.

1. Introduction

Li-air battery has nearly the highest theoretical energy density among chemical energy storage systems and could be the final solution for various applications, such as electrical vehicles, robots, aircrafts [1]. It has been demonstrated that the catalyst loaded air electrode could decrease the overpotentials of the carbon electrode for both discharging (oxygen reduction reaction, ORR) and charging (oxygen evolution reaction, OER, in addition to decomposition of formed discharging products) processes. Intensive efforts have been paid to explore high efficient and low cost catalysts for both the ORR and the OER reactions in Li-air batteries. Many materials such as transitional metal oxides [2–4] i.e., MnO_2, Fe_3O_4, CuO, $CoFe_2O_4$ and noble metal Pt [5,6], and nanocomposites [7–9] such as Pd/MnO_2 have been demonstrated as efficient catalysts only for the OER process. Some catalysts such as metal Au and FeCu/C [10,11] have shown activity only for the ORR process. Nanocomposite PtAu was found to be a unique good bifunctional electrocatalyst. However, it is expensive for large scale applications. In most cases, the catalysts are loaded on large surface area carbon particles and the air electrodes contain binders and conductive additives. It is difficult to deconvolute the functions of non-carbon catalyst and carbon substrate [5]. In addition, detecting the spatial distribution of discharge products is essential for understanding the features of the air electrode and improving its performance, however, it is hard to be performed for complicated powder electrode. In this paper, we demonstrate that the cobalt oxide (CoO_x)/diamond-like carbon (DLC) double-layer electrode is a low cost and high efficient catalyst for nonaqueous Li-air cells. Based on secondary ion mass spectrometry (SIMS) detection, the spatial distribution of discharge products in the active layer is revealed in Li-air cell with carbonate based electrolyte. The CoO_x/DLC double

* Corresponding author. Tel.: +86 21 65642422; fax: +86 21 65102777.
E-mail address: zwfu@fudan.edu.cn (Z.-W. Fu).

0378-7753/$ – see front matter © 2012 Elsevier B.V. All rights reserved.
http://dx.doi.org/10.1016/j.jpowsour.2012.09.052

layer electrode presented both high OER catalytic activity and excellent cycling performance in ether based electrolyte, making it a promising candidate for cathode material in Li-air batteries.

2. Experimental

2.1. Preparation of CoO_x/DLC

The preparation of the DLC thin film air electrode is described in our recent work [12]. The DLC thin film was deposited on the silicon substrate by radio frequency (RF) sputtering method using a carbon target (purity of 99.999%). The island-like CoO_x thin film was deposited onto the surface of the DLC layer by a pulsed laser deposition (PLD) method using CoO (purity of 99.99%) target. A 355 nm laser beam provided by the third harmonic frequency of a Q-switched Nd: yttrium aluminum garnet laser (Spectra Physics GCR-150) with a pulsed repetition rate of 10 Hz and a pulsed width of 5 ns was focused onto the surface of the target. The incident angle between the laser beam and the target surface normal was 45°. The laser intensity was about 2 J cm^{-2}. The distance between the target and substrate was 30 mm. The pressure of the high-purity Ar ambient gas was controlled at 5–10 Pa by a needle valve during deposition. The films were deposited on a silicon-DLC substrate at 450 °C. The cross-sectional scanning electron microscopy (SEM) image of the as-deposited CoO_x/DLC thin films shows that the thicknesses of the DLC and the CoO_x layer in this double-layer electrode were about 1000 nm and 90 nm, respectively.

2.2. Electrochemical cell and analysis

The model cell consisted of an H shape glass tube to separate positive and negative electrodes as well as two rubber plugs for sealing. The cell was constructed with the thin film as the cathode and one sheet of high-purity lithium foil as the anode, respectively. The electrolyte was 1 M $LiPF_6$ non-aqueous solution in ethylene carbonate (EC) and dimethyl carbonate (DMC) with a volume ratio of 1:1 (Merck). Recent studies have demonstrated that in carbonate based electrolyte, cycling of Li-air battery is based on decomposition of electrolyte solvent forming lithium alkyl carbonates during discharge process and oxidative decomposition of these discharge products upon charge process [13,14]. Therefore, electrocatalysts in air cathode for carbonate based Li-air cell actually catalyze the formation and decomposition of lithium alkyl carbonates rather than lithium oxide/peroxide. Herein, we also employed this CoO_x/DLC double layer electrode in 1,2-dimethoxyethane (DME) based electrolyte (1 M LiTFSI in DME), which has been proved more stable to oxygen reduced species than carbonate based electrolyte [15,16], to testify its electrocatalytic activity for ORR and OER. The discharge and charge processes were performed at room temperature with a Land BT 1–40 battery test system. When the cells were cycled in the containers, the dried air diffused into the electrolyte solution spontaneously and supported the cycling of the cells. The current densities and capacities of electrodes were calculated based on the weight of DLC.

2.3. Physical and morphology measurements

Weight of thin film was directly obtained by subtracting the original substrate weight from total weight of the substrate and deposited thin film onto its surface, which were examined by electrobalance (BP 211D, Sartorius). The precision of the weight was ±0.01 mg. The morphologies of the thin film electrodes were examined by a scanning electron microscopy (SEM) (Cambridge S-360). X-ray photoelectron spectroscopy (XPS) measurements were performed on a Perkin Elmer PHI 6000C ECSA system with monochromatic Al Kα (1486.6 eV) irradiation. To correct possible charging of the films by X-ray irradiation, the binding energy was calibrated using the C1s (284.6 eV) spectrum of hydrocarbon that remained in the XPS analysis chamber as a contaminant. High resolution transmission electron microscopy (HR-TEM) and selected area electron diffraction (SAED) measurements were carried out on a JEOL 2010 TEM at 160 kV accelerating voltage. Fourier transform infrared (FTIR) spectra were recorded on a Nicolet Nexus-470 spectrometer. Secondary ion mass spectrometry (SIMS) depth profiling was made with a Cameca IMS-3f SIMS spectrometer. An oxygen beam with an 8 keV impact energy was rastered over a 200 × 200 μm region and the secondary ion signals were collected from the center of the sputtered area over an area with a 60 μm diam.

3. Results and discussion

Fig. 1 shows the TEM and SAED images of the as-deposited electrode. It can be clearly observed from Fig. 1(a) that the dark spots, assigned to the CoO_x nanoparticles, distribute in the nano-structured DLC matrix. The CoO_x nanoparticles have an average

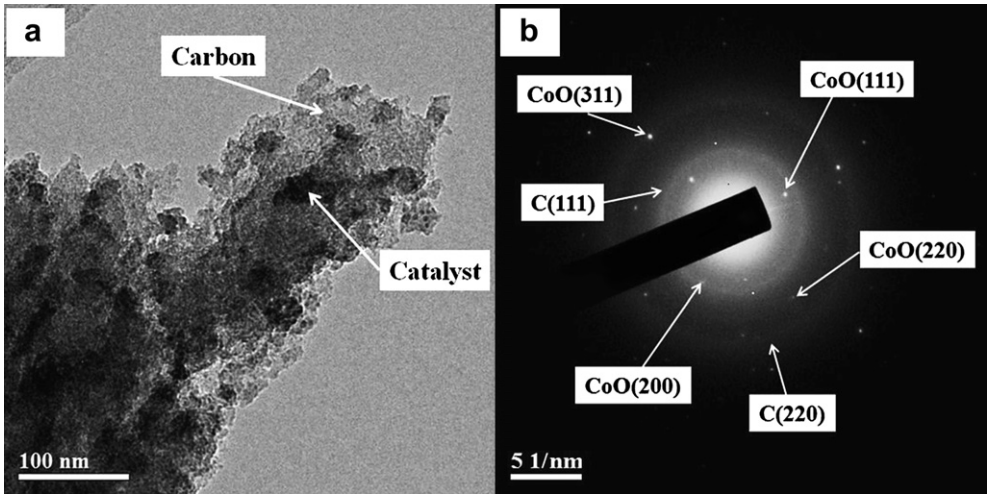

Fig. 1. (a) TEM image and (b) SAED patterns of the as-deposited CoO_x/DLC thin film electrode.

Table 1
d-Spacings (Å) derived from SAED analysis of the as-deposited, the discharged CoO_x/DLC thin film electrode in DME based electrolyte. JCPDS standards of diamond carbon, CoO_x and Li_2O_2 are shown for references.

As-deposited					
TW[a]	Diamond carbon (89-3441) $Fd\bar{3}m$	TW	CoO (78-0431) $Fm\bar{3}m$		
		2.46	2.46 (111)		
2.10	2.06 (111)	2.13	2.13 (200)		
1.26	1.26 (220)	1.55	1.51 (220)		
		1.29	1.29 (311)		
$a = 3.60 \pm 0.03$	$a = 3.57$	$a = 4.29 \pm 0.09$	$a = 4.26$		
First discharging to 2.0 V in DME based electrode					
TW	Diamond carbon (89-3441) $Fd\bar{3}m$	TW	CoO (78-0431) $Fm\bar{3}m$	TW	Li_2O_2 (09-0355) $P\bar{6}$
2.08	2.06 (111)	2.44	2.46 (111)	2.56	2.56 (101)
		2.13	2.13 (200)	1.21	1.22 (114)
1.23	1.26 (220)	1.50	1.51(220)	1.04	1.02 (211)
		1.28	1.29(311)	0.94	0.95 (213)
$a = 3.51 \pm 0.09$	$a = 3.57$	$a = 4.24 \pm 0.02$	$a = 4.26$	$a = 3.15 \pm 0.05$ $c = 7.66 \pm 0.03$	$a = 3.14$ $c = 7.65$

[a] TW: this work.

diameter of around 20–40 nm. The SAED pattern in this region is presented in Fig. 1(b). Two clear and weak rings could be indexed to the face-centered cubic structure of diamond carbon (JCPDS card no. 89-3441). Besides, many bright discrete diffraction spots also exist in the SAED patterns. All d-spacings derived from the SAED patterns are shown in Table 1. These discrete diffraction spots can be indexed to the face-centered cubic structure of CoO (JCPDS card no. 78-0431), which unambiguously confirm the top layer is CoO.

Fig. 2 presents Co 2p and O 1s XPS spectra of the as-deposited CoO_x/DLC thin film electrode. As shown in Fig. 2(a), the Co $2p_{3/2}$ binding energy peak at 780.4 eV, the Co $2p_{1/2}$ binding energy peak at 796.2 eV and two intense shake-up satellite peaks at 785.4 and 801.8 eV are observed, respectively. According to literature data [17], they can be attributed to Co 2p binding energy for CoO. This result is in good agreement with the TEM and SAED data (Fig. 1). In Fig. 2(b), O 1s XPS spectra can be deconvoluted into three components peaked at 529.6 eV (O_I, 17.7%), 530.6eV (O_{II}, 73.5%) and 532.1eV (O_{III}, 8.9%). Species O_I has the commonly observed BE of oxygen adsorbed on transition metals placed in sites referring to the metal oxide, and therefore it is associated with the stoichiometric oxygen in CoO, while O_{III} is ascribed to surface contamination [18]. For the O_{II} species, it can be assigned to low-coordinated oxygen ions at the surface, grain boundaries and other defect sites which do not fit the crystallographic requirements of stoichiometric cobalt oxide [19]. From the relatively large intensity of the O_{II} component (73.5%), it can be concluded that the as-deposited cobalt oxide film should mainly consists of CoO with a significant amount of defects (CoO_x, $x < 1$), and the surface of CoO_x film can absorb oxygen molecules (O_{III}).

In order to compare the catalytic effect of CoO_x/DLC double-layer electrode with former reported catalysts, electrochemical measurement of air electrodes were first performed in carbonate based electrolyte. Fig. 3 shows the initial discharge/charge curves of the DLC and the CoO_x/DLC thin film electrodes in EC/DMC based electrolyte under one atm dried air and 2 atm oxygen, respectively. Both cells were cycled at constant current density of 100 mA g^{-1} (0.017 mA cm^{-2}) between 2.0 V and 4.3 V. Under one atm dried air, the open circuit voltages (OCV) of the DLC electrode and the CoO_x/DLC electrode are 3.00 V and 3.14 V, respectively. The DLC electrode and the CoO_x/DLC electrode show similar voltage profiles and deliver initial discharge capacity of 450 and 824 mAh g^{-1}, respectively. The average discharge voltage plateau of the CoO_x/DLC electrode is 2.72 V, which is about 100 mV higher than 2.62 V of the DLC electrode. Higher discharge capacity and lower discharge overpotential clearly indicate that the adding of the CoO_x top layer can enhance the activity of discharge process significantly. For the initial charge process, the charging voltage profiles show a hump at early stage and then increase steadily. The appearance of the hump is related to the sluggish diffusion and reaction kinetics of the charging process for thin film air electrode [12]. The charging of the DLC electrode starts at 3.9 V after the hump region. The average voltage is about 4.2 V and its charge capacity is 309 mAh g^{-1}. The charging of the CoO_x/DLC electrode starts at 3.6 V and the average charging voltage is about 4.12 V. The corresponding capacity is 795 mAh g^{-1}, which is 96.5% of its initial discharge capacity. These results preliminarily indicate that CoO_x/DLC double layer has positive effects both for discharge and charge processes in EC/DMC based electrolyte.

In order to understand the reaction behaviors further, two cells with the DLC and the CoO_x/DLC electrodes under oxygen partial pressure of 2 atm oxygen were investigated. As shown in Fig. 3, the average discharge plateau of the DLC electrode under 2 atm oxygen is 2.69 V (70 mV higher than that in 1 atm air) and the initial discharge capacity is 598 mAh g^{-1}. It means that the kinetics of the discharge reaction in the DLC electrode is limited by the adsorption and diffusion of oxygen. This is reasonable for the discharge reaction and consistent with Yang's conclusion [20]. However, the average discharge plateau of the CoO_x/DLC under 2 atm oxygen is

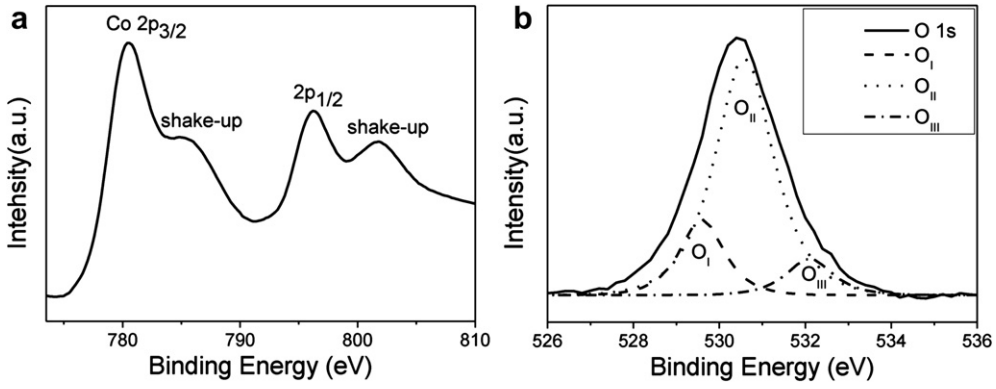

Fig. 2. (a) Co 2p and (b) O 1s XPS spectra of the as-deposited CoO_x/DLC thin film electrode.

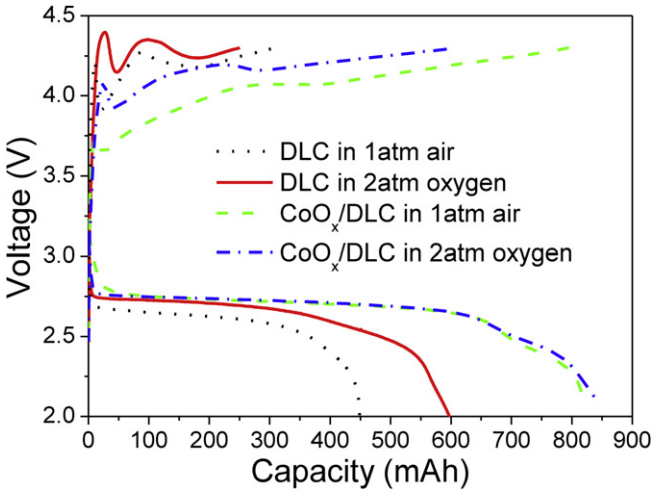

Fig. 3. The initial discharge/charge curves of the DLC and CoO_x/DLC thin film electrodes/Li air cells in EC/DMC based electrolyte cycled between 2.0 V and 4.3 V at the current densities of 100 mA g^{-1} under the condition of one atm dried air and 2 atm oxygen, respectively.

almost identical with that under 1 atm air and the capacity does not increase significantly. Apparently, the higher oxygen pressure can significantly improve the discharge process of DLC, but do not affect the discharge process of the CoO_x/DLC. This means that the rate determining step for the CoO_x/DLC electrode in 1atm air is not related to the adsorption and diffusion of oxygen. In other words, the CoO_x seems to ensure the same oxygen concentration at the active sites of the DLC thin film in 1 atm air as that in 2atm oxygen. It is believed that a significant amount of defects in the CoO_x layer (concluded from XPS results) and at the CoO_x/DLC interface from the strain should be beneficial to the adsorption and exchange kinetics of dissolved oxygen molecules from the electrolyte to the active sites of DLC thin film, thus enrich the higher oxygen concentration around DLC thin film even under lower dissolved oxygen concentration of electrolyte. For the charge process, the average charge plateaus of both the DLC and the CoO_x/DLC electrodes shift to higher position after changing the cell working ambient from 1 atm air to 2 atm oxygen. This indicates that the voltage polarization increases in both cases under higher oxygen pressure. This is also reasonable for the charge reaction.

As many researchers have pointed out, Li_2CO_3/Li alkyl carbonates are the dominate discharge products in carbonate-based electrolytes [13,14]. In this work, thin films were deposited on the double-sided polishing silicon for FTIR tests to detect discharge products and the results are presented in Fig. 4(a). Compared to FTIR spectra of as deposited thin film, some new peaks appear in FTIR spectra of the discharged electrode. The peaks at 867 cm^{-1}, 1436 cm^{-1} and 1502 cm^{-1} (labeled by the asterisks) can be assigned to Li_2CO_3. The peaks at 1186 cm^{-1}, 1774 cm^{-1} and 1801 cm^{-1} (labeled by the hollow circles) can be assigned to asymmetric and symmetric stretching vibrations of lithium alkyl carbonate ($ROCO_2Li$). FTIR data suggests that the main discharge products are amorphous Li_2CO_3 and $ROCO_2Li$ when the electrode is discharged to 2.0 V in the carbonate electrolyte.

While loads of investigations are focusing on various electrochemical transport parameters which affect the discharge profiles, there are few studies trying to understand the spatial distribution of discharge products in Li-air battery because this is relatively difficult for powder electrodes. Herein we use SIMS technique to study the spatial distribution of discharge products in carbonate based Li-air cell, which is of great significance to design air

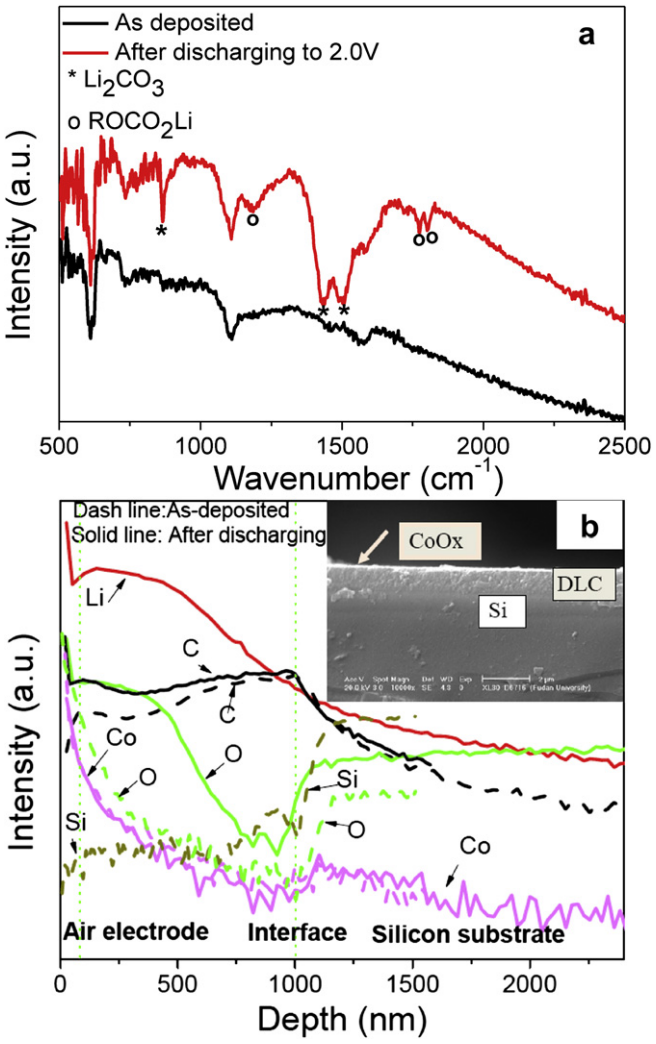

Fig. 4. (a) FTIR spectra of the pristine CoO_x/DLC thin film electrode and the electrode after discharging to 2.0 V in EC/DMC based electrolyte; (b) SIMS depth profiles of C, Co, O and Si atom for the as-deposited CoO_x/DLC thin film and C, Co, Li, O distribution profiles after discharging the corresponding Li-air cell to 2.0 V in EC/DMC based electrolyte. The thickness of the DLC layer is approximately 1000 nm from the cross-sectional SEM image shown in the inset.

electrode ideal for Li-air chemistry. The SIMS depth profiles of C, Co, O and Si atoms for the as-deposited CoO_x/DLC thin film and C, Co, Li, O distribution profiles for the CoO_x/DLC thin film after discharging to 2.0 V in EC/DMC based electrolyte are shown in Fig. 4(b). The curves of the as-deposited sample show that the concentration of Co decreases quickly with increase of the SIMS sputtering time while the concentration of C changes oppositely. After the depth reaches around 90 nm from the surface of the air electrode (marked at the left dash line), the concentration of C atom stays almost unchanged. These results consist with the SEM cross-section image of the double-layer feature (inset of Fig. 4(b)). After discharging, the distributions of Co atoms are almost the same as the as-deposited sample. It means that Co atoms do not diffuse during the discharge reaction.

The depth profiles of Li, C and O atoms after discharging are also shown in Fig. 4(b). P and F have not been detected by SIMS, indicating the absence of the residual lithium salt from the electrolyte on the surface of the electrode. It is noticed that the concentration of C and O atom of the discharged electrode is higher than that of the initial electrode with the appearance of the depth profile of Li

after the discharge. Furthermore, the depth profile of O atom below the depth of 500 nm is nearly identical to that of Li atom after discharging, supporting that oxygen and Li ions diffuses into the CoO_x/DLC film to form discharge products such as Li_2CO_3 and $ROCO_2Li$ during discharge process. Noteworthily, this is the first time to use SIMS technique to demonstrate the main discharge products are Li_2CO_3 and $ROCO_2Li$ in carbonate-based electrolyte.

Interestingly, it can be seen that most discharge products generates from the interface to about half depth of the DLC layer (~500 nm), and neither at the interface between the electrolyte and CoO_x layer or at the interface between CoO_x and DLC layers. Apparently, the reaction active sites is mainly distributed inside the DLC thin film, and the optimized thickness of DLC layer should be approximate 500 nm for 90 nm thick CoO_x layer, which can greatly increase the utilization of the DLC film, thus double the present gravimetric discharge capacity in the CoO_x/DLC air batteries. This result provides important information for guiding the design and fabrication of the catalyzed air cathode with the suitable size ratio of loaded catalyst to the substrate in Li air batteries. In addition, the outside of CoO_x layer is not coated by the discharge products, indicating that this double-layer structure can avoid the catalyst surface blocked by the discharge products, resulting in the catalytic inactivity.

In aiming of studying the catalytic effect of CoO_x/DLC electrode on oxygen reduction and evolution electrochemistry, the electrochemical characterization of a DME-based Li-air cell was tested using CoO_x/DLC thin film electrode in comparison with carbonate based Li-air cell. Fig. 5 presents the initial discharge/charge curves of the DLC and the CoO_x/DLC thin film electrodes in DME based electrolyte under 1 atm dried air and 2 atm oxygen, respectively. Both cells were cycled at constant current density of 100 mA g^{-1} (0.017 mA cm^{-2}). Different from the results in EC/DMC based electrolyte under 1 atm dried air ambient (Fig. 3), DLC electrode and the CoO_x/DLC electrode in DME based electrolyte show similar voltage profiles and deliver initial discharge capacity of approximately 2500 mAh g^{-1}. The average discharge voltage plateaus of both electrodes are around 2.78 V. This can be explained by the fact that both solubility of O_2 and oxygen diffusion coefficient in DME solvent are much higher than those in carbonate solvent [21,22]. As a result, concentration and transportation of O_2 in air electrode at

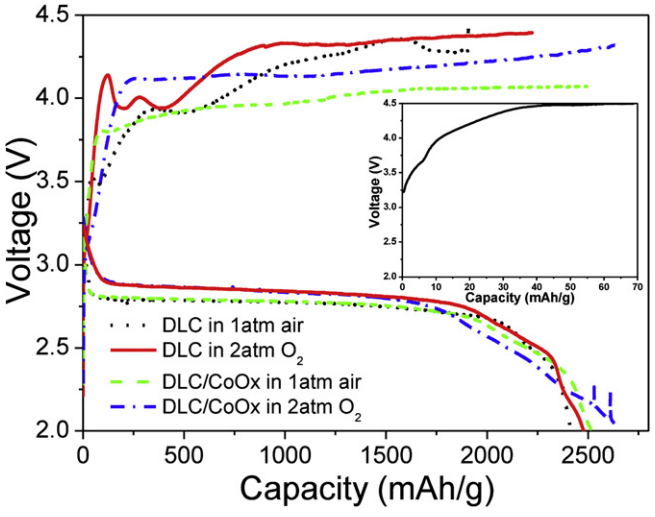

Fig. 5. The initial discharge/charge curves of the DLC and CoO_x/DLC thin film electrodes/Li air cells in DME based electrolyte cycled at the current densities of 100 mA g^{-1} under the condition of one atm dried air and 2 atm oxygen, respectively. The inset shows charge voltage profile of CoO_x/DLC thin film electrode during the first charge from OCV to 4.5 V at 100 mA g^{-1}.

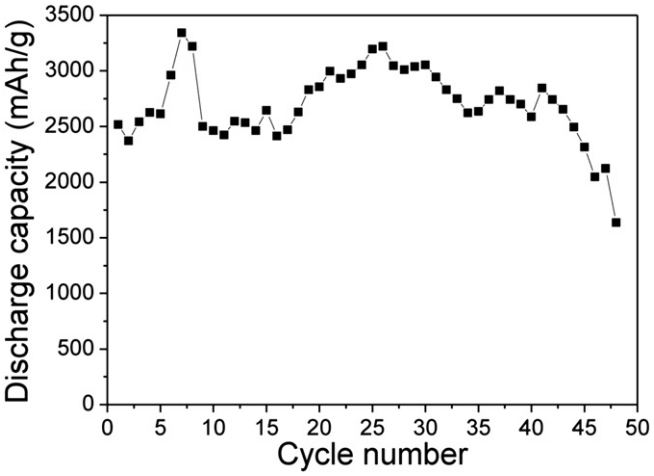

Fig. 6. The cycling performance of Li-air cell using CoO_x/DLC thin film air electrode at current density of 100 mA g^{-1} in DME based electrolyte.

low current density (100 mA g^{-1}) are no longer key factors which might limit performance of the electrode. So the function of enriching adsorption and diffusion of oxygen into the bottom DLC in EC/DMC based electrolyte when discharging by CoO_x layer seems to be ineffective in DME based electrolyte, causing almost identical discharge capacities and overpotentials in DME based electrolyte.

For the initial charge process, however, things become different for the two electrodes. The average charge voltage plateau of DLC electrode is ~4.24 V while that of DLC/CoO_x electrode is 3.98 V, 260 mV lower. In order to exclude that the charging voltage is a result of electrolyte decomposition, the first charge from OCV of the cell with DLC/CoO_x as electrode to 4.5 V was tested and the result is shown in the inset of Fig. 5. From the charge curve, it is clear that side charge reactions associated with electrolyte decomposition was quite negligible (less than 40 mAh g^{-1} charge capacity below 4.4 V), which unambiguously demonstrated that charge voltage plateau corresponded to OER process. This data indicates that CoO_x has pretty high catalytic activity for OER, corresponding to the decomposition of Li_2O_2.

When the two types of electrodes are enclosed into an oxygen box and run under 2 atm O_2, it is not surprised both the discharge and charge voltage plateaus shifted to higher positions, just like those in EC/DMC based electrolyte. The discharge voltages of two electrodes are still identical and the value is 2.84 V while the charge voltages of DLC electrode and DLC/CoO_x are 4.32 V and 4.15 V, respectively.

Another phenomenon worth noting is that the capacities of both two electrodes in 1 atm air and 2 atm O_2 are nearly the same, around 2500 mAh g^{-1}. In DME based electrolyte, concentration and transportation of O_2 in the air electrode are sufficient enough to sustain ORR process during discharge at low current density of 100 mA g^{-1}, so the available space in the electrode to accommodate discharge products determines the discharge capacity of the electrode. Given that CoO_x layer and improving oxygen pressure do not introduce new available space in DLC, the discharge capacities stay almost unchanged for both electrodes in higher oxygen pressure.

The cyclic performance of the DLC/CoO_x electrode in DME based electrolyte was also conducted and the result is shown in Fig. 6. The discharge test was carried out at the rate of 100 mA g^{-1} with cutoff voltage of 2.0 V; the charge test was performed under the same current density and was terminated when the capacity reached 2500 mAh g^{-1}. It can be observed from the figure that the capacity retention of DLC/CoO_x electrode is fairly excellent. The initial

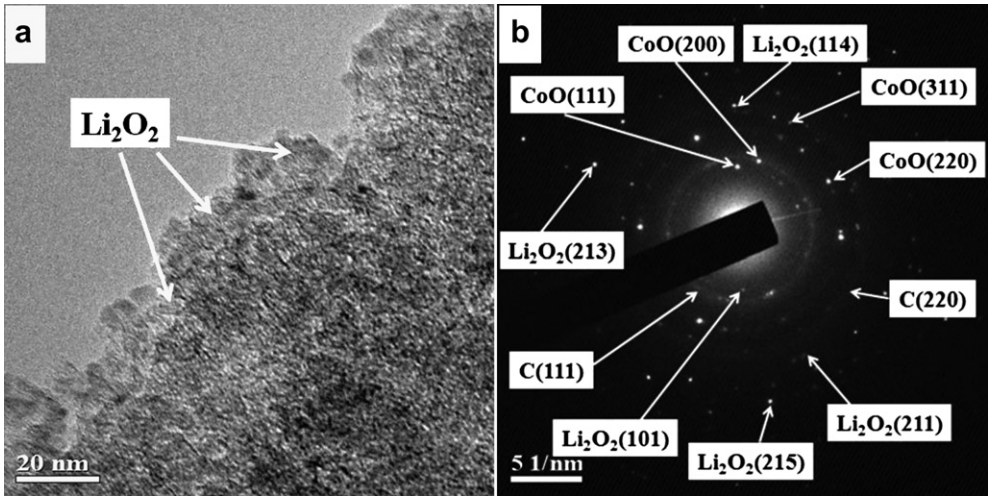

Fig. 7. (a) TEM image and (b) SAED patterns of the CoO_x/DLC thin film electrode after discharging to 2.0 V at the first cycle in DME based electrolyte.

discharge capacity is 2518 mAh g^{-1} based on the weight of DLC, after 44th cycles the discharge capacity remains at 2500 mAh g^{-1} with some fluctuation during cycling. Afterwards, the cell performance began to fail. According to Bruce's research, ether solvents are gradually attacked by reduced oxygen species and decompose with further cycling although they are much more stable than carbonate solvents, leading to the accumulation of discharge products in the cathode [15]. As a result, fading of the air electrode occurs. The cycling performance of the CoO_x/DLC double-layer air electrode is among the best state-of-the-art air electrodes reported [3–9,23–26].

In order to identify the reaction products on the CoO_x/DLC electrode in DME based electrolytes, we performed the TEM and SAED measurements on the cathode after the CoO_x/DLC thin film electrode discharging to 2.0 V and the results are shown in Fig. 7. It can be observed from TEM images that thin films of discharge products precipitated and attached onto the carbon matrix, as labeled by the white arrow. SAED pattern of this region confirms the existence of hexagonal Li_2O_2 (JCPDS 09-0355) besides diamond carbon and CoO in the discharged electrode. All d-spacings derived from the SAED spectra are shown in Table 1. This result show that unlike Li-air cells operating in EC/DMC based electrolyte, Li_2O_2 is the dominant discharge products on the cathode in DME based electrolyte, which is consist with other researchers' conclusions [22,27].

Based on the above results in DME based Li-air cell, the scheme of the catalytic effects of CoO_x layers for charge process is shown in Fig. 8. As we discussed above, in EC/DMC based electrolyte, the existence of the CoO_x top layer could not only enrich oxygen molecules at the active sites of DLC thin film to enhance discharge reaction activity during the discharge process but also have a high catalytic activity for the decomposition of discharge products (Li_2CO_3 and $ROCO_2Li$) during charge process. While for Li-air cell in DME based electrolyte, the enrichment of oxygen at DLC active sites during discharge process through CoO_x layer is not so apparent since oxygen solubility and diffusivity in DME is sufficient to sustain ORR. However, CoO_x thin film seems to have high electrocatalytic activity for decomposition of Li_2O_2.

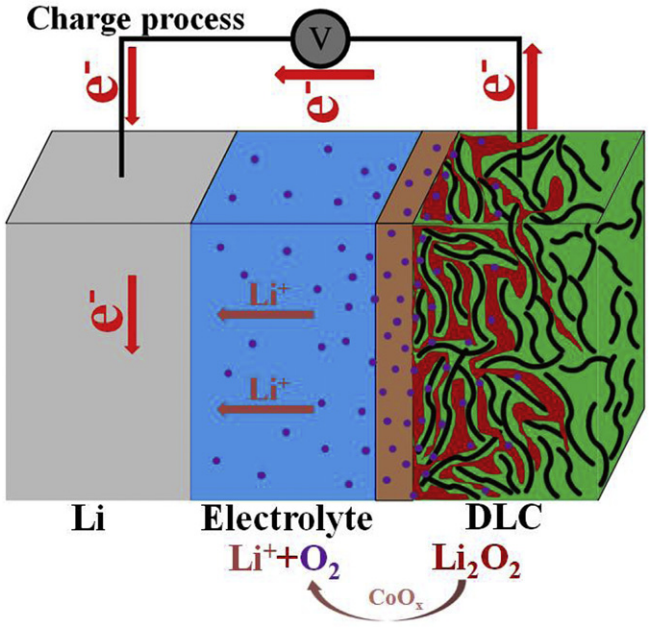

Fig. 8. Schematic diagram of CoO_x/DLC thin film air electrode for Li/air battery during charge process in DME based electrolyte.

4. Conclusions

In this work, a CoO_x layer with the thickness of around 90 nm was deposited onto the DLC thin film (~1000 nm) by PLD technique and this double-layer structure thin film was used as the air cathode for both EC/DMC and DME based Li-air batteries. A EC/DMC based Li-air cell using a CoO_x/DLC double-layer thin film air electrode shows great improvement for discharge/charge overpotentials. SIMS technique was firstly used to determine the composition as well as spatial distribution profile of discharge products in EC/DMC based electrolyte. The CoO_x/DLC double-layer air in DME based electrolyte exhibits high electrocatalytic activity towards OER, lowering the charge overpotential of ~260 mV. In addition, over 40 cycles with high capacity of more than 2000 mAh g^{-1} was achieved. Our results indicate that CoO_x/DLC double-layer thin film air electrode is a promising candidate for rechargeable Li-air batteries of high energy density.

Acknowledgements

This work was financially supported by Science & Technology Commission of Shanghai Municipality (08DZ2270500 and 09JC1401300) and 973 Program (No.2011CB933300) of China.

References

[1] C.X. Zu, H. Li, Energy Environ. Sci. 4 (2011) 2614–2624.
[2] T. Ogasawara, A. Debart, M. Holzapfel, P. Novak, P.G. Bruce, J. Am. Chem. Soc. 128 (2006) 1390–1393.
[3] A. Debart, A.J. Paterson, J. Bao, P.G. Bruce, Angew. Chem. 120 (2008) 4597–4600.
[4] A. Debart, J. Bao, G. Armstrong, P.G. Bruce, J. Power Sources 174 (2007) 1177–1182.
[5] Y.C. Lu, H.A. Gasteiger, E. Crumlin, R. McGuire Jr., Y. Shao-Horn, J. Electrochem. Soc. 157 (2010) A1016–A1025.
[6] Y.C. Lu, H.A. Gasteiger, M.C. Parent, V. Chiloyan, Y. Shao-Horn, Electrochem. Solid State Lett. 13 (2010) A69–A72.
[7] Y.C. Lu, Z. Xu, H.A. Gasteiger, S. Chen, K. Hamad-Schifferli, Y. Shao-Horn, J. Am. Chem. Soc. 132 (2010) 12170–12171.
[8] A.K. Thapa, K. Saimen, T. Ishihara, Electrochem. Solid State Lett. 13 (2010) A165–A167.
[9] A.K. Thapa, T. Ishihara, J. Power Sources 196 (2011) 7016–7020.
[10] S.S. Zhang, X. Ren, J. Read. Electrochim. Acta 56 (2011) 4544–4548.
[11] X. Ren, S.S. Zhang, D.T. Tran, J. Read, J. Mater. Chem. 21 (2011) 10118–10125.
[12] Y. Yang, Q. Sun, Y.S. Li, H. Li, Z.W. Fu, J. Electrochem. Soc. 158 (2011) B1211–B1216.
[13] W. Xu, K. Xu, V.V. Viswanathan, S.A. Towne, J.S. Hardy, J. Xiao, Z. Nie, D. Hu, D. Wang, J.G. Zhang, J. Power Sources 196 (2011) 9631–9639.
[14] S.A. Freunberger, Y. Chen, Z. Peng, J.M. Griffin, L.J. Hardwick, F. Bard, P. Novak, P.G. Bruce, J. Am. Chem. Soc. 133 (2011) 8040–8047.
[15] S.A. Freunberger, Y. Chen, N.E. Drewett, L.J. Hardwick, F. Barde, P.G. Bruce, Angew. Chem. Int. Ed. 50 (2011) 1–6.
[16] H. Wang, K. Xie, Electrochim. Acta 64 (2012) 29–34.
[17] T.J. Chuang, C.R. Brund, D.W. Rice, Surf. Sci. 59 (1976) 413–429.
[18] S. Valeri, A. Borghi, G.C. Gazzadi, A. di Bona, Surf. Sci. 423 (1999) 346–356.
[19] V.M. Jimenez, A. Fernandez, J.P. Espinos, A.R. Gonzalez-Elipe, J. Electron. Spectrosc. Relat. Phenom. 71 (1995) 61–71.
[20] X. Yang, Y. Xia, J. Solid State Electrochem. 14 (2010) 109–114.
[21] J. Read, K. Mutolo, M. Ervin, W. Behl, J. Wolfenstine, A. Driedger, D. Foster, J. Electrochem. Soc. 150 (2003) A1351–A1356.
[22] Y.-C. Lu, D.G. Kwabi, K.P.C. Yao, J.R. Harding, J. Zhou, L. Zuind, Y. Shao-Horn, Energy Environ. Sci. 4 (2011) 2999–3007.
[23] B. Sun, B. Wang, D. Su, L. Xiao, H. Ahn, G. Wang, Carbon 50 (2012) 727–733.
[24] H. Cheng, K. Scott, J. Power Sources 195 (2010) 1370–1374.
[25] H. Wang, Y. Yang, Y. Liang, G. Zheng, Y. Li, Y. Cui, H. Dai, Energy Environ. Sci. 5 (2012) 7931–7935.
[26] L. Zhang, X. Zhang, Z. Wang, J. Xu, D. Xu, L. Wang, Chem. Commun. 48 (2012) 7598–7600.
[27] B.D. McCloskey, D.S. Bethune, R.M. Shelby, G. Girishkumar, A.C. Luntz, J. Phys. Chem. Lett. 2 (2011) 1161–1166.